A Concept of Multiphase Dynamic Charging System with Constant Output Power for Electric Vehicles

Van-Binh Vu
School of Engineering
Newcastle University
Newcastle upon Tyne, UK
v.b.vu2@ncl.ac.uk

Mohamed Dahidah
School of Engineering
Newcastle University
Newcastle upon Tyne, UK
mohamed.dahidah@ncl.ac.uk

Volker Pickert
School of Engineering
Newcastle University
Newcastle upon Tyne, UK
volker.pickert@ncl.ac.uk

Van-Tung Phan
School of Engineering
Newcastle University
Newcastle upon Tyne, UK
vantung.phan@ncl.ac.uk

***Abstract*— Dynamic changing of Electric Vehicles (EV) is a new initiative aimed at increasing EV uptake. However, pulsating output power along driving direction is one of the most serious problems of such technology. This paper proposes a new configuration that ensures constant power with minimum power electronics requirements. The proposed system utilizes multiple primary windings that guarantee a homogeneous mutual magnetic flux for the receiver along the driving direction. This results in a constant induced voltage and hence constant output power to charge the EV's battery. Structure layout for primary transmitters including ferrite cores and windings is suggested and theoretical analysis is conducted to draw conditions of each winding's current phase and amplitude for achieving constant output power. The effectiveness of the proposed system is analytically demonstrated and experimentally verified using a 3-kW laboratory prototype with three-phase system.**

Keywords— Dynamic Wireless Charging, Multiphase system, Electric Vehicle Battery Charger, Constant Output Power.

I. INTRODUCTION

Electric vehicles (EV) have recently received a great deal of attention because of their clean, efficient and environment-friendly features [1]. However, the high penetration of EVs still limited at present time due to several technological barriers, including battery capacity. It is normally required to equip an expensive and large battery with long charging time to achieve satisfactory EV driving range. To address this problem, the concept of WDC has been proposed in [2] to overcome the limitation of current battery technology. WDC enables EV to be charged wirelessly while in motion. As a result, the battery size of EVs can be greatly reduced and the driving range limitation can be completely alleviated. WDC is commonly developed based on inductive power transfer (IPT) technology, where a time varying magnetic field is generated by transmitter coils; which are installed underneath road surface, to wirelessly power receiver coils, which charging the EV's battery continuously [3]-[5].

A WDC are categorized into short-individual transmitters [6-8] or long-track transmitter [9-11] according to the length of transmitter coils. In the short-individual transmitters, the transmitter's dimension is commonly the same as the receiver. Multiple transmitter coils are arranged in the primary side to alternatively transfer power to secondary side. When the EV's receiver is in align with a specific transmitter, then the power switch connects the associated inverter. Short-track transmitter has advantageous of low electromagnetic field level and high efficiency as minimizing conduction loss on transmitter winding. However, when the EV moves between two adjacent transmitters, the output power becomes pulsating and significantly reduces.

On the other hand, long-track transmitter [9-11] is much longer than the EV's length and only requires a single power inverter with one compensation tank. This brings benefits in terms of cost and simplicity for implementation of such a system. Nevertheless, the efficiency is reduced and electromagnetic interference (EMI) is increased. Several studies are conducted to address EMI problem and also to simplify the structure of the system [12-14] by adopting alternative magnetic polarity to construct transmitters. However, these studies also pointed out that the magnetic flux density generated by primary transmitter on a receiver varies in a nearly sinusoidal function depending on receiver's position along the driving direction. Consequently, the induced voltage and received power are significantly varied depending on EV's position. The received output power even reaches to nearly zero at some specific position of EV while moving along the transmitter.

Several studies were carried out to attain constant output power for both short and long-track system. These methods include (1) optimization of resonant tanks [15-16], (2) optimization of transmitter and receiver's dimensions [17] and (3) using multiple transmitters [14] or receiver [18]. However, they require either complex control or design procedures.

This paper introduces a generalized concept to achieve a constant output power by using a multiphase transmitter system applying for long-track transmitter type. The transmitter system is constructed using multiple magnetic poles with different polarities and multiple windings. Multiphase inverter is adopted to produce the required currents (i.e. amplitude and phase) for each transmitter's winding. The paper presents a generalized multiphase system, however the number of phases is selected based on the required output power. The proposed concept is validated with an illustrative example based on a three-phase system. A scale down laboratory prototype of 3-kW is developed to experimentally verify the feasibility and effectiveness of the proposed system. The results indicate that almost constant output power is achieved when receiver in motion along the driving direction.

II. Analysis of The Proposed Multiphase WDC

A. The circuit configuration

Fig. 1 depicts the proposed multiple transmitters WDC aiming to attain constant output power for an EV's dynamic charging system. Primary side consists of n transmitters L_i ($i = 1,2,\ldots,n$) energizing one receiver coil, L_s. As these transmitters are physically placed closed to each other, therefore crossing couplings exists between windings as depicted in Fig. 1. The mutual inductances between transmitter L_i and receiver is denoted by M_{is} ($i = 1,2,\ldots,n$). A multi-phase DC/AC inverter is used at the primary side to produce a high frequency AC voltage for each transmitter. The switching frequency of the inverter is chosen as 85 kHz according to SAE J2954 standard. Each transmitter is driven by a constant current source regardless of load and coupling coefficient conditions. In order to produce constant transmitter's current I_i ($i = 1,2,\ldots,n$), the resonance between L_{ia} and C_{ia} is set at the switching frequency of the inverter. The series capacitors C_{ib} ($i = 1,2,\ldots,n$) are used for resonating with the transmitter's inductance L_{ia} and suppressing the induced voltages caused by the crossing couplings from other transmitters. At the secondary side, another LCC resonant tank is connected with a full-bridge rectifier to provide DC power to the output load. The proposed layout of primary transmitters and conditions of transmitter currents are further detailed in the following subsections. It is worth noting that the configuration in Fig. 1 is only applicable with minimum number of phases (n) of three. However, when n equals to 2, the proposed system can be configured by using two conventional half-bridge converters for two phases.

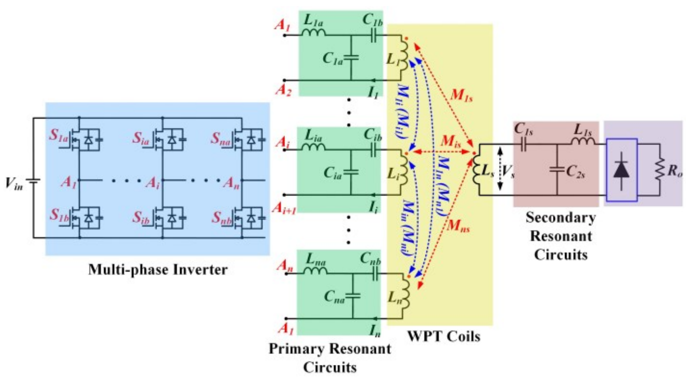

Fig. 1. The proposed circuit of dynamic charging system with multiple transmitter coils.

B. Issue of single phase transmitter system

Fig. 2(a) shows WDC system consisting of multiple alternating magnetic I-pole core, where the receiver is covering one magnetic pole. When receiver is perfectly aligned with center of each magnetic pole, (i.e. completely covers the winding loop), then mutual inductance will reach its maximum value. On the other hand, the mutual inductance drops to zero when the receiver centered at the middle point between each adjacent poles, where the magnetic fluxes cancel each other (i.e. same magnitude but opposite directions), resulting in no induced voltage. Therefore, as the receiver (EV) moves along the transmitter, spatial periodic induced voltage (V_s) and power (P_o) are obtained, which both are proportional with mutual inductance value. Consequently, as the vehicle travels along transmitter, the battery will not receive any power at the points of zero-mutual-inductance (i.e. *pulsating power*). The spatial distribution of mutual inductance between a single transmitter and receiver can be approximately expressed by (1). The measured and simulated mutual inductance for 2.4m and 4-pole single transmitter system are portrayed in Fig 2(b).

$$M_{1s}(x) = M_o \sin\left(\frac{2\pi x}{l_o}\right) \tag{1}$$

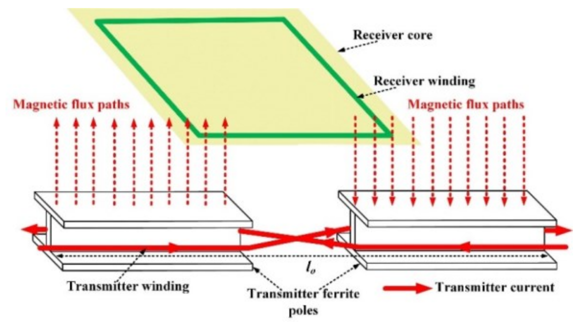

(a)

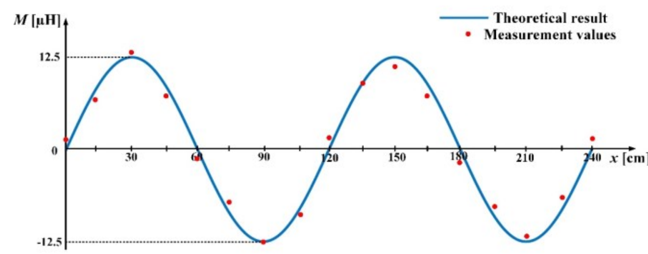

(b)

Fig. 2. Single transmitter system (a) Side view when receiver positions in lowest mutual inductance point (b) Spatial distribution of mutual inductances

C. The layout of the proposed multiple transmitters

The derivation of the proposed layout is inspired by the limitations of a single transmitter systems. In order to solve abovementioned problems, additional transmitters can be added into the original system to nullify the zero mutual inductance points. The number of additional transmitters is determined by the output power requirement volt-ampere capability of the system components such as power switches, transmitter coil and resonant capacitors. To attain a constant output power, it is essential to ensure that the additional mutual inductances M_{ks} ($k = 2,3,\ldots,n$) are evenly distributed along the transmitter length to avoid any zero mutual inductance points. It refers that between any two adjacent null points of $M_{1s}(x)$, there are new $n-1$ null points from added mutual inductances. In other words, the phase difference between any two adjacent mutual inductances $M_{ks}(x)$ and $M_{(k+1)s}(x)$ should be equal as illustrated in Fig. 3. It is also avoided to add new null points of M_{ks} ($k = 2,3,\ldots,n$) into the same positions with existing one of $M_{1s}(x)$, otherwise, added $M_{ks}(x)$ does not contribute to compensate the null-point of $M_{1s}(x)$. The phase-shift difference between any two adjacent mutual inductance curves $M_{ks}(x)$ and $M_{(k+1)s}(x)$ is set at π/n. Equation (2) expresses all n mutual inductances (i.e. $M_{is}(x)$ ($i = 1,2,\ldots,n$).

$$
\begin{cases}
M_{1s}(x) = M_o \sin\left(\frac{2\pi x}{l_o}\right) \\
M_{2s}(x) = M_o \sin\left(\frac{2\pi x}{l_o} - \frac{\pi}{n}\right) \\
\vdots \\
M_{is}(x) = M_o \sin\left[\frac{2\pi x}{l_o} - (i-1)\frac{\pi}{n}\right] \\
\vdots \\
M_{ns}(x) = M_o \sin\left[\frac{2\pi x}{l_o} - (n-1)\frac{\pi}{n}\right]
\end{cases} \tag{2}
$$

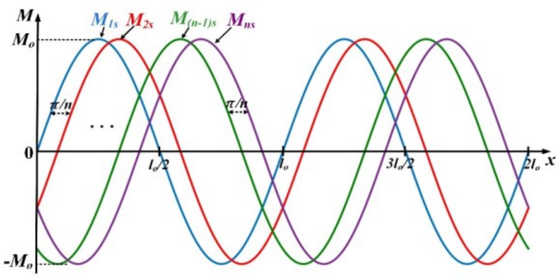

Fig. 3. Expected spatial distribution of mutual inductances for the proposed multiple transmitters

In order to obtain evenly distributed $M_{is}(x)$ as shown in (2), the proposed n transmitters is structured as depicted in Fig. 4, which is based on I-type ferrite shape as presented in [12]. As discussed above, $n-1$ additional mutual inductances are evenly distributed over the length of $l_o/2$. Furthermore, in the proposed system, each original core of the conventional single transmitter is divided into n small cores. These small cores dimensions are adjustable and determined by the application requirements.

In addition, as the multiple transmitter windings of the proposed system are placed close to each other, therefore there will be crossing mutual inductance between them. These cause higher currents stresses through the inverter switches as well as resonant components and have destructive effects on the inverter switches. To solve this effect, a small capacitor is connected in series with each transmitter to cancel the induced voltages caused by the cross coupling.

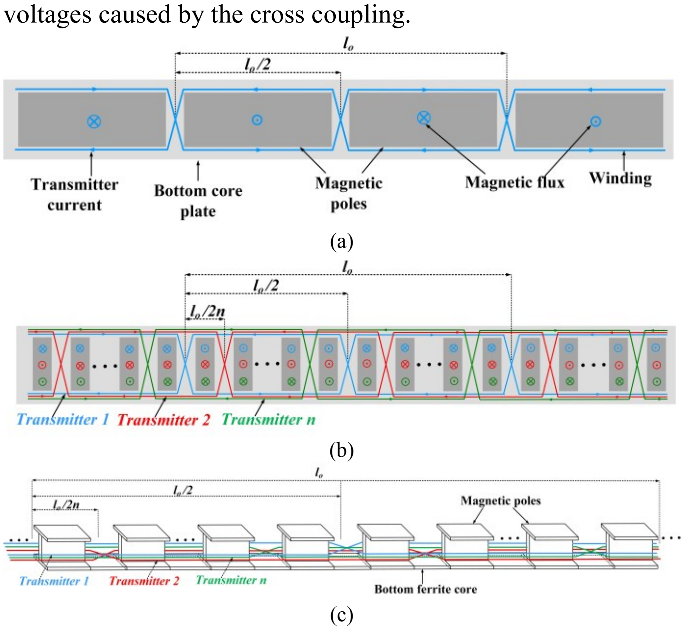

Fig. 4 Layout configuration of (a) Conventional single transmitter [12] (b) Top view and (c) Side view of the proposed multiple transmitters

III. CONDITIONS OF ACHIEVING CONSTANT OUTPUT POWER

The open-circuit induced voltage V_s on the receiver can be written by:

$$
V_s = j\omega \sum_{i=1}^{n} M_{is}(x) I_i \tag{3}
$$

Where I_i is the current through transmitter i and $M_{is}(x)$ is the mutual inductance between transmitter i and the receiver.

Assuming the inverter produces equal voltages (i.e. with phase shift of π/n) across each resonant tank, therefore the currents through transmitter windings can be expressed by:

$$
\begin{cases}
I_1 = I_o e^{j0} \\
I_2 = I_o e^{j\frac{\pi}{n}} \\
\vdots \\
I_i = I_o e^{j(i-1)\frac{\pi}{n}} \\
\vdots \\
I_n = I_o e^{j(n-1)\frac{\pi}{n}}
\end{cases} \tag{4}
$$

Consequently, V_s can be further expressed as follows:

$$
\begin{aligned}
|V_s| &= \omega \left| \sum_{i=1}^{n} M_o \sin\left(\frac{2\pi x}{l_o} - (i-1)\frac{\pi}{n}\right) I_o\, e^{j(i-1)\frac{\pi}{n}} \right| \\
|V_s| &= \omega M_o I_o \left| \sum_{i=1}^{n} \left\{ \frac{e^{j\left[\frac{2\pi x}{l_o} - (i-1)\frac{\pi}{n}\right]} - e^{-j\left[\frac{2\pi x}{l_o} - (i-1)\frac{\pi}{n}\right]}}{2j} \right\} e^{j(i-1)\frac{\pi}{n}} \right| \\
|V_s| &= \frac{\omega M_o I_o}{2} \left| \sum_{i=1}^{n} e^{j\frac{2\pi x}{l_o}} - e^{-j\frac{2\pi x}{l_o}} \sum_{i=1}^{n} e^{j(i-1)\frac{2\pi}{n}} \right|
\end{aligned} \tag{5}
$$

Where:

$$
\sum_{i=1}^{n} e^{j(i-1)\frac{2\pi}{n}} = 1 + Z_1 + Z_1^2 + Z_1^3 + \cdots + Z_1^{n-1} = \frac{1 - Z_1^n}{1 - Z_1} = 0 \tag{6}
$$

In (6) $Z_1 = e^{j(2\pi/n)}$. Considering (6), the final expression of $|V_s|$ is given as:

$$
|V_s| = \frac{\omega M_o I_o}{2} \left| n e^{j\frac{2\pi x}{l_o}} - 0 \right| = \frac{n\omega M_o I_o}{2} \tag{7}
$$

A conclusion can be drawn by (7) that the induced voltage is constant regardless of receiver's position if adopting the transmitter's layout with expression of mutual inductances in (2) and condition for transmitter's current is shown in (4). This value of $|V_s|$ and related output power P_o are proportional to number of transmitters n, angular inverter frequency ω, amplitude I_o of transmitter's currents as well the maximum value of M_o. Depending on required power level and allowed implementing cost, these above factors should be considered carefully in design procedure.

IV. EXPERIMENTAL VERIFICATIONS

The proposed multi-phase system is validated with an illustrative example based on a three-phase system in this Section. The conventional three-phase inverter is adopted in primary side. The proposed layout in Fig. 4 is applied with $n=3$ and a small modification is made as shown in Fig. 5(a) by reversing order between transmitter 2 and 3 to match with the phases of three-phase inverter output voltage. Therefore the phase difference between two consecutive transmitters is set as $2\pi/3$. The laboratory prototype of 3-kW is designed and implemented. As shown in Fig. 5(a), the transmitter windings are arranged in three layer, which isolated from each other using plastic sheets. Furthermore, Kapton-tape-shield Litz wire is used to further improve the isolation winnings different loops of the same phase's winding. The receiver shown in Fig. 5(b) and the dimension of the receiver is 60cm x 60cm while the maximum air-gap between the transmitter and receiver is tested at 15 cm.

The detailed system specification is depicted in Table I. C_{com1}, C_{com2}, C_{com3} are connected in series with transmitters winding to suppress induced voltages caused by crossing mutual inductances M_{12}, M_{13}, M_{23}. The tests were conducted when receiver moves along transmitter in driving direction.

TABLE II
SPECIFICATION AND PARAMETERS OF THE PROPOSED WDC

Symbol	Parameter	Value
V_{in}	Input voltage	400 V
I_o	Rated output current	6.5 A
P_o	Rated output power	3 kW
L_1, L_2, L_3	Self-inductance of transmitters	182 µH
L_s	Self-inductance of receiver	118 µH
M_o	Maximum mutual inductance	12.5 µH
M_{12}, M_{13}, M_{23}	Crossing mutual inductances	-46 µH
L_{1a}, L_{2a}, L_{3a}	Primary additional inductors	37 µH
C_{1a}, C_{2a}, C_{3a}	Primary parallel capacitors	95 nF
C_{1b}, C_{2b}, C_{3b}	Primary series capacitors (without compensated capacitors)	24.2 nF
C_{com1}, C_{com2}, C_{com3}	Primary compensated capacitors	76.22 nF
L_{1s}	Secondary additional inductors	35 µH
C_{2s}	Secondary parallel capacitors	100 nF
C_{1s}	Secondary series capacitors	42.2 nF
f	Switching frequency	85 kHz

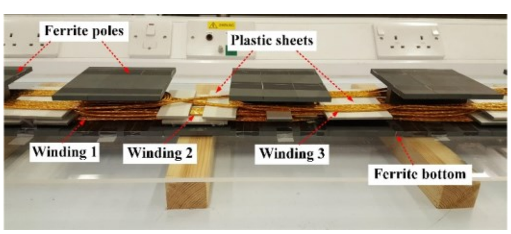

(a)

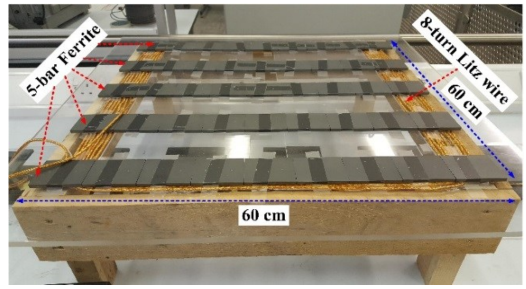

(b)

Fig. 5. Experimental test-rig of the three-phase WDC system (a) Three-phase transmitter (b) Receiver

Fig. 6 illustrates key operating waveforms at the primary side circuit. Specifically, Fig. 6(a) presents the output voltages V_{12}, V_{23} and V_{31} while transmitter currents I_1, I_2 and I_3 can be seen in Fig. 6(b). I_1, I_2 and I_3 have the same amplitude and a phase-shift of 120 degrees apart from each other.

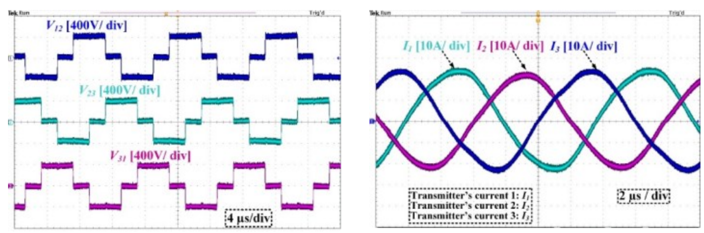

(a) (b)

Fig. 6. (a) Primary inverter's voltage (b) Transmitter's currents

Fig. 7 further demonstrates the operation of the proposed system under different loading conditions (i.e. 40Ω and 70Ω) while receiver is in the moving process. Moreover, the harvested output power at different positions along the driving direction x as portrayed in Fig. 8. It should be noted that receiver's displacement x starts only from 15cm and ends at 225cm as only cases when the whole receiver is positioned on the transmitter windings are considered.

The power fluctuation factor is defined as $\Delta P = \left(\frac{P_{max}-P_{min}}{P_{max}}\right) * 100\%$. For this particular experiment, ΔP are found to be 4.9 %, 5.6 % and 5.1 % with the load of 17, 40 and 70 Ω, respectively. It can be considered that constant output power is achieved with the proposed system.

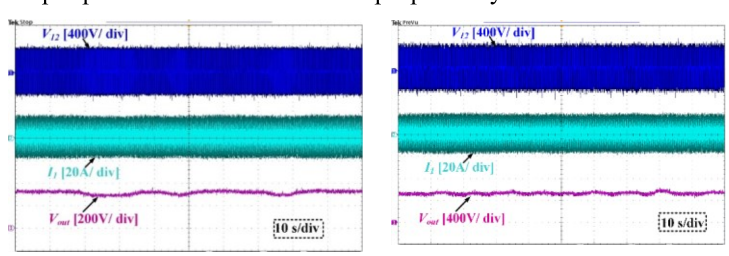

(a) (b)

Fig. 7. Experimental waveforms with different load while receiver moving along driving direction (a) R_o = 40 Ω, (b) R_o = 70 Ω

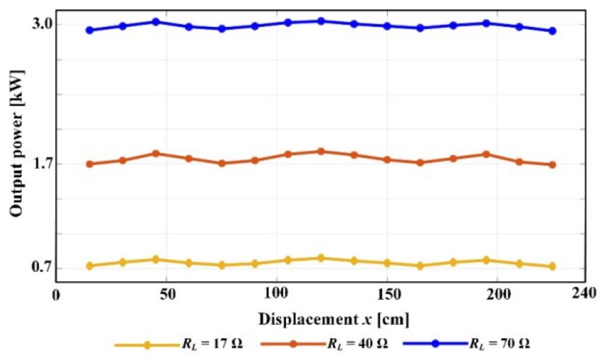

Fig. 8. Measured output power with different load conditions and different receiver positions along the driving direction

V. CONCLUSIONS

This paper proposes a generalized concept to attain constant output power while EV is in motion along the driving direction aiming for high power WDC system. The concept adopts multiple windings combining with alternative ferrite poles in primary side to effectively produce a constant coupling magnetic flux between transmitters and receiver. The detailed layout for transmitter as well as conditions of transmitter current are provided.

For illustration, the experimental results of three phase system WDC are presented. With a 3 kW laboratory prototype, the tests at different conditions of load and receiver displacements were conducted. The power fluctuation factor at rated load can attain 5.6% when receiver moves along driving direction of transmitters.

REFERENCES

[1] M. Yilmaz and P. T. Krein, "Review of battery charger topologies, charging power levels, and infrastructure for plug-in electric and hybrid vehicles," IEEE Trans. Power Electron., vol. 28, no. 5, pp. 2151–2169, May 2013.

[2] S. Y. Choi , B. W. Gu , S. Y. Jeong , C. T. Rim "Advances in Wireless Power Transfer Systems for Roadway-Powered Electric Vehicles," *IEEE J. Emerg. Sel. Topics Power Electron.,* vol. 3, no. 1, pp. 18-36, Mar. 2015.

[3] D. H. Tran, V. B. Vu and W. J. Choi, "Design of a High Efficiency Wireless Power Transfer System with Intermediate Coils for the On-board Chargers of Electric Vehicles," IEEE Trans. Power Electron., vol. 33, no. 1, pp. 175–187, Jan. 2018.

[4] V. B. Vu, D. H. Tran and W. J. Choi, "Implementation of the Constant Current and Constant Voltage Charge of Inductive Power Transfer Systems with the Double-Sided LCC Compensation Topology for Electric Vehicle Battery Charge Applications," IEEE Trans. Power Electron., IEEE Trans. Power Electron., vol. 33, no. 9, pp. 7398 - 7410,Sep. 2018.

[5] V. B. Vu, V. T. Phan, M. Dahidah and V. Pickert, "Multiple Output Inductive Charger for Electric Vehicles," IEEE Trans. Power Electron., to appear.

[6] G. A. Covic and J. T. Boys, "Modern trends in inductive power transfer for transportation applications," IEEE Trans. Emerg. Sel. Topics Power Electron., vol. 1, no. 1, pp. 28–41, Mar. 2013.

[7] Q. Zhu, L. Wang, Y. Guo, C. Liao, and F. Li, "Applying LCC compensation network to dynamic wireless EV charging system," IEEE Trans. Ind. Electron., vol. 63, no. 10, pp. 6557–6567, Oct. 2016.

[8] J. M. Miller, O. C. Onar, C. P. White, and S. Campbell, "Demonstrating dynamic wireless charging of an electric vehicle: The benefit of electrochemical capacitor smoothing," *IEEE Power Electron. Mag.,* vol. 1, no. 1, pp. 12–24, Mar. 2014

[9] J. Shin et al., "Design and implementation of shaped magnetic resonance based wireless power transfer system for roadway-powered moving electric vehicles," *IEEE Trans. Ind. Electron*., vol. 61, no. 3, pp. 1179–1192, Mar. 2014.

[10] B.-M. Song, R. Kratz, and S. Gurol, "Contactless inductive power pickup system for Maglev applications," in Proc. 37th IEEE IAS Annu. Meeting, Oct. 13–18, 2002, vol. 3, pp. 1586–1591.

[11] W. Y. Lee et al., "Finite-width magnetic mirror models of mono and dual coils for wireless electric vehicles," *IEEE Trans. Power Electron*., vol. 28, no. 3, pp. 1413–1428, Mar. 2013.

[12] J. Huh, S. W. Lee, W. Y. Lee, G. H. Cho, and C. T. Rim, "Narrow-width inductive power transfer system for on-line electrical vehicles (OLEV)," *IEEE Trans. Power Electron*., vol. 26, no. 12, pp. 3666–3679, Dec. 2011.

[13] S. Y. Choi, S. Y. Jeong, B. W. Gu, G. C. Lim, and C. T. Rim, "Ultraslim S-type power supply rails for roadway-powered electric vehicles," *IEEE Trans. Power Electron*., vol. 30, no. 11, pp. 6456–6468, Nov. 2015.

[14] C. Park, S. Lee, S. Jeong, G.-H. Cho, and C. Rim, "Uniform power I-type inductive power transfer system with DQ-power supply rails for on-line electric vehicles," *IEEE Trans. Power Electron*., vol. 30, no. 11, pp. 6446– 6455, Nov. 2015.

[15] J. Zhao, T. Cai, S. Duan, H. Feng, C. Chen, and X. Zhang, "A General Design Method of Primary Compensation Network for Dynamic WPT System Maintaining Stable Transmission Power," *IEEE Transactions on Power Electronics*, vol. 31, no. 12, pp. 8343-8358, Dec. 2016.

[16] H. Feng, T. Cai, S. Duan, J. Zhao, X. Zhang, and C. Chen, "An LCC-compensated resonant converter optimized for robust reaction to large coupling variation in dynamic wireless power transfer," IEEE Trans. Ind. Electron., vol. 63, no. 10, pp. 6591–6601, Oct. 2016.

[17] F. Lu, H. Zhang, H. Hofmann, and C. C. Mi, "A dynamic charging system with reduced output power pulsation for electric vehicles," IEEE Trans. Ind. Electron., vol. 63, no. 10, pp. 6580–6590, Oct. 2016.

[18] S. Cui, Z. Wang, S. Han, C. Zhu and C. C. Chan, "Analysis and Design of Multiphase Receiver with Reduction of Output Fluctuation for EV Dynamic Wireless Charging System," IEEE Trans. Power Electron., to appear.